

Variable Power, Short Microwave Pulses Generation using a CW Magnetron

Vasile SURDUCAN¹, Emanoil SURDUCAN¹, Radu CIUPA²

¹National Institute for Research and Development of Isotopic and Molecular Technology, 65-103 Donath St., Cluj-Napoca, 400483, Romania, ²Technical University Cluj-Napoca, Romania
vasile.surduncan@itim-cj.ro

Abstract—Fine control of microwave power radiation in medical and scientific applications is a challenging task. Since a commercial Continuous Wave (CW) magnetron is the most inexpensive microwave device available today on the market, it becomes the best candidate for a microwave power generator used in medical diathermy and hyperthermia treatments or high efficiency chemical reactions using microwave reactors as well. This article presents a new method for driving a CW magnetron with short pulses, using a modified commercial Zero Voltage Switching (ZVS) inverter, software driven by a custom embedded system. The microwave power generator designed with this method can be programmed for output microwave pulses down to 1% of the magnetron's power and allows microwave low frequency pulse modulation in the range of human brain electrical activity, intended for medical applications. Microwave output power continuous control is also possible with the magnetron running in the oscillating area, using a dual frequency Pulse Width Modulation (PWM), where the low frequency PWM pulse is modulating a higher resonant frequency required by the ZVS inverter's transformer. The method presented allows a continuous control of both power and energy (duty-cycle) at the inverter's output.

Index Terms—Continuous Wave Magnetron, Pulse Width Modulation, Zero Voltage Switching, Microcontroller, Microwave Pulse Modulation.

I. INTRODUCTION

Microwaves are electromagnetic radiations in the frequency range of 300MHz and 300GHz, named also centimeter waves. Microwave power radiation is widely used in medical applications such as microwave diathermy or microwave hyperthermia. The control of a temperature rise generated by the microwave power deposition into the tissue [1] is expressed in (1):

$$\frac{\Delta T}{\Delta t} = \frac{1}{2} \frac{\sigma}{\rho c} (E_{rms}^2 - C_{he}) \quad (1)$$

where the tissue temperature increase (ΔT) in a microwave thermal procedure is proportional with the microwave power deposition into the tissue (E_{rms}^2) and the irradiation time (Δt) (assuming the tissue is described by quasi-constant parameters during the treatment time: σ -conductivity, ρ -density, c -specific heat, C_{he} -convection heat exchange term from the Pennes approximation). The boundary between the non-thermal and thermal effect produced by a microwave radiation is debatable [2]; however, the maximum limit value accepted is the whole body average SAR = 4, (Specific Absorption Rate) or a long term exposure to a microwave power density of 50W/m². If

a microwave non-thermal effect occurs, the temperature increase of the body must be less than 0.2°C-0.3°C as measured on an average irradiation time of 6 minutes. As seen in (1), the effect of low microwave power can be equilibrated by the human body reaction (it can be entirely compensated by the blood flow) and the local effect of the microwave irradiation becomes non-thermal. Non-thermal effects of the microwaves can stimulate the patient's brain activity during the treatment if the microwave field is modulated with a specific frequency.

When both thermal and non-thermal effects are requested during a microwave treatment, the driving system of a microwave generator must control the microwave power, the treatment time and the microwave energy deposition with very good precision, allowing the use of a high microwave power source for generating higher or lower intensity radiations, as demanded. The CW commercial magnetron (and its conventional power supply) is not suitable, as it is, for low microwave power generation. For example, the home appliance magnetron supply [3] is controlling the magnetron's energy in ON-OFF sequences, using the magnetron's maximum output power pulses. Such a supply method can not be used safely for medical applications, where too much power in the microwave pulse can produce irreversible damages (burns) to the tissues. Microwave pulses are inducing into the tissue biomolecular dipolar displacement, free charge current or/and higher resonant absorption than continuous microwave radiation. An improved supply solution is either the usage of a multi-coil transformer, supplying the magnetron's anodic voltage with a determined pulse sequence [4] or a smart drive of the magnetron's inverter supply, which allows a dynamic output power control.

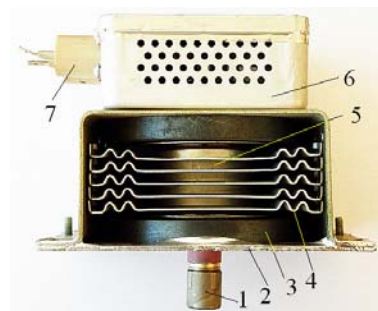


Figure 1. Magnetron aspect: 1-antenna, 2-mounting plate, 3-magnet, 4-heatsink, 5-anode, 6-filter box, 7-cathode and filament terminals.

II. MAGNETRON OPERATION

The first magnetron was invented back in 1921 by the

American physicist Albert Hull [5] at General Electric.

However, the first resonant cavity magnetron, similar with those used nowadays (Fig. 1), was developed in 1935 by the German physicist Hans Hollman [6] at Telefunken. A magnetron is a high power microwave oscillator in which the potential energy of an electron cloud near the cathode is converted into microwave energy in a series of cavity resonators. The safety working area (Fig. 2) of a magnetron with a permanent magnet is determined by the magnetic induction ΔB_m , dictated by the value of the maximum anode voltage variation ΔU_0 . The working area in the cylindrical magnetron model [7], is defined between Hull's parabola (2) and the synchronization line (3):

$$B_0^2 = \frac{4U_0 \cdot \frac{2m}{e}}{d^2 \left(1 + \frac{\rho_c}{\rho_a}\right)^2} \tag{2}$$

$$U_0 \approx \frac{4\pi f}{N} \cdot d \cdot \rho_c \cdot B_0 \tag{3}$$

Where: U_0 = anodic voltage [V], B_0 = magnetic field[G], $e = 1.60210 \cdot 10^{-19}$ [C], electron charge, $m = 9.109 \cdot 10^{-31}$ [Kg], electron mass, $d = \rho_a - \rho_c$ cathode to anode distance [m], ρ_c = cathode diameter [m], ρ_a = anode diameter [m], f = microwave frequency [Hz], N = number of the resonant cavities.

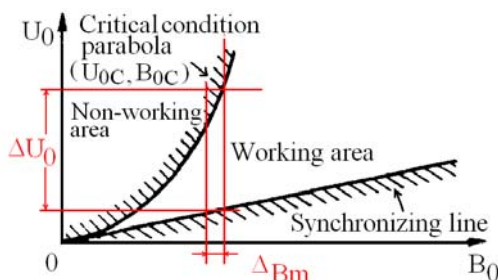


Figure 2. The safety working area of a magnetron: U_{0c} -critical anode voltage, B_{0c} -critical magnetic field.

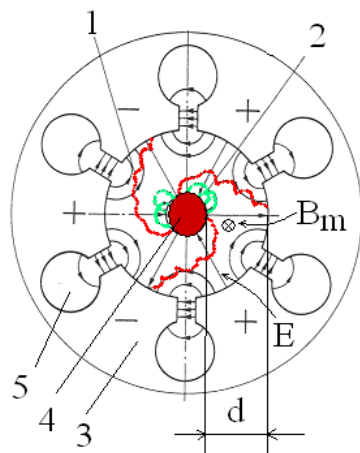


Figure 3. Cross-section schematic of the working magnetron: 1-the spatial charge rotor, 2-“lost” electrons, 3-anode, 4-cathode, 5-resonant cavity, d = anode-cathode distance, E -electric field, B_m -magnetic field.

Once the heater and anodic voltage are turned on, electrons leave the heated cathode and are accelerated

toward the anode. The presence of a strong magnetic field B_m (Fig. 3) in the region between cathode and anode produces a force on each electron which is perpendicular to the electron velocity vectors, causing the electrons to spiral away from the cathode in paths of various types of cycloids, depending upon the initial electron velocity. The cloud of electrons approaching the anode interacts with the microwave field created in the resonators and the electrons will either be slowed, if interacting with an opposing microwave field, or accelerated, if they are in the vicinity of an aiding microwave field. The slowed electrons will drift toward the anode while the accelerated electrons will curl back away from the anode. The result is a cloud of electrons grouped in a spatial charge rotor with each spoke located at a resonator having an opposing microwave field. On each half cycle of the oscillation, the radiofrequency field pattern will change its polarity and the spoke pattern of the spatial charge rotor will rotate to maintain its presence in an opposing field. The microwave energy maintained by the spatial charge rotor is collected through a feeder to the magnetron's antenna. The synchronism between the electron spoke pattern and the radiofrequency field polarity (Fig. 3) allows a magnetron to maintain a stable operation above the synchronization area (Fig. 2) if the filament current and a correct anodic voltage is sustained.

The static characteristic of the 2450MHz/1200W CW magnetron (Fig. 4) is quasi-similar to a high voltage Zener diode.

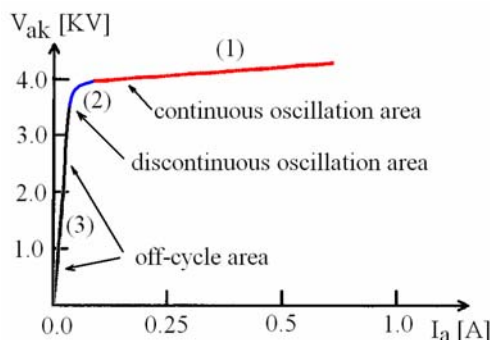


Figure 4. Experimental characteristic of a CW magnetron.

The cut-off voltage varies between 3.5KV (700W magnetrons) to 4KV (1200W magnetrons) for different commercial manufacturers. The magnetron efficiency varies around the value of 75%. In discontinuous oscillation area, the magnetron still oscillates if the anode voltage is slowly decreased from typical 4.5KV until the cut-off voltage is reached.

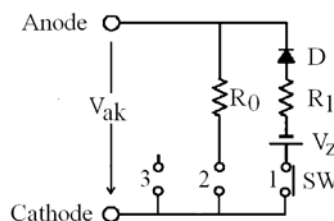


Figure 5. Electrical equivalent circuit model of magnetron.

Once the magnetron is off, it can be turned on again only if supplied with the minimum anode voltage corresponding to

the continuous oscillation area. This behavior makes difficult controlling the magnetron output power in the discontinuous oscillation area, which in practice is an avoided situation.

In the oscillating area, the voltage can be considered almost constant (it is a linear voltage-current characteristic, with small slope) and the microwave power of the magnetron is proportional to its anode current. In the off-cycle area the anode current becomes zero. The equivalent electrical model (Fig. 5) of the magnetron is shown running in the continuous oscillation area (1) (see Fig. 4), where $R_1 \approx 250..300$ ohm and $R_0 = V_{ak}/I_a$. Both R_0 and R_1 are pure resistors, D is an ideal diode, V_z an ideal battery (the cut-off voltage) and SW an ideal switch. If the inverter output current capability is limited, once the magnetron runs in the oscillating area, a voltage drop may appear.

III. QUASI-RESONANT ZERO VOLTAGE SWITCHING INVERTER

The active clamp quasi-resonant zero voltage switching inverter (ZVS), pulse width (PWM) and pulse frequency modulated (PFM) structure (Fig. 6) comprises a main switch IGBT Q1 and a sub-switch Q2, both feeding a step-up transformer through a voltage resonant switching circuit (Q2, C2, C1). Detailed switching algorithm of the circuit is described in [8]-[11]. The main switch is driven from a logic driver module, supplied from the main voltage through D3, D4 and R4 and synchronized with the zero cross power supply voltage. The logic module analyses the Q1 collector amplitude voltage and the zero voltage switching time and reads the current flow through TR1 using a current transformer TR2. The sub-switch has a passive network which acts as a signal forming and driver, Q2 being driven by the Q1 collector voltage. In this way Q1 and Q2 are turned ON and OFF with 180° phase shifting. The switching frequency is around 30 KHz, reduced to 25-26 KHz during ZVS period if PFM is active. The energy W transferred into the TR1 is:

$$W = V_{dc}^2 \cdot t_{onH}^2 / 2L \quad (4)$$

Where: V_{dc} = power supply voltage [V], t_{onH} = turn on switching time [s], L = transformer inductivity [H].

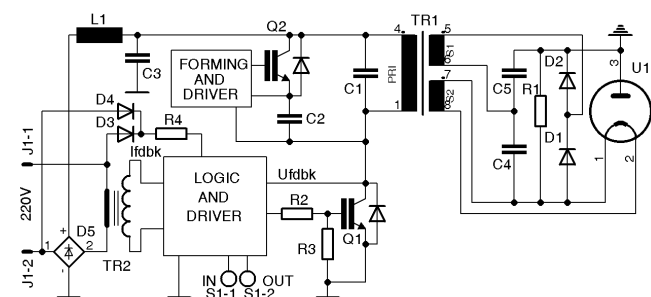


Figure 6. The standard ZVS inverter structure.

Modifying t_{onH} controls the output anode current through the magnetron U1, while the output voltage at TR1 secondary is rectified and doubled through D1, D2 and C4, C5. Measuring U_{fdbk} , the logic circuit holds the Q1 collector voltage below 800V. The logic module driving Q1 has an

opto-isolated input S1-1 and an opto-isolated output S1-2. The input signal is turning ON the inverter, while the output is keeping the track of the ON time of the main switch driver output.

TABLE I. ZVC ESSENTIAL COMPONENTS SPECIFICATIONS

Q1	Q2	C1	C2
Uc:1KV Ic:60A tf:0.25µs	Uc:0.6KV Ic:30A tf:0.25µs	0.1µF/400V	0.45µF/400V
TR1	D1, D2	C4, C5	R1
PRI:120µH S1: 28mH S2: 0.49µH	8KV/350mA tf:0.15 µs	8.2nF/3KV	100M/4KV

Where: U_c = collector voltage, I_c = collector current, t_f = forward switching time.

Two essential problems are encountered when using this inverter in medical applications:

1. The shortest high voltage pulse width at the inverter output is too large (Fig. 7), the finest microwave operational efficiency range (5) is 14% at $f_{PWM} = 1$ Hz; use of higher PWM frequencies is not possible because of huge resolution loss.
2. Acquiring short microwave pulses at the magnetron output is impossible because the magnetron filament regime time is minimum 5s and the filament is supplied from the same anode voltage transformer.

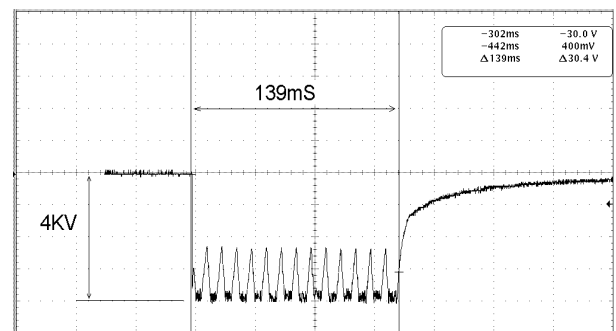


Figure 7. Output voltage of the ZVS inverter, with 1ms input driving pulse on S1-1.

IV. SOFTWARE PATTERN MODULATION

The classic inverter uses for the switching logic a custom master slice IC of bipolar process, with fixed modulation algorithms. Obtaining various types of pulse patterns and controlling the anodic current is possible using a programmable custom embedded design [12]. A dual PWM modulation pattern has been implemented (Fig. 8). The lower frequency PWM (F_{PWML}) needed for microwave pulse

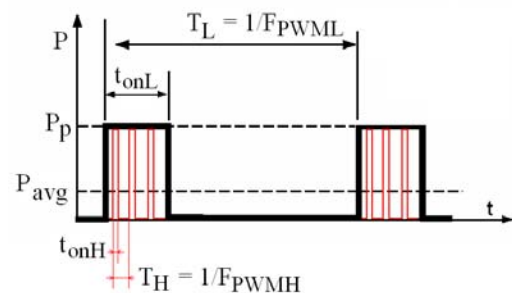


Figure 8. Dual PWM modulation technique, where: $\delta_L = t_{onL}/T_L$ low frequency (PWML) duty cycle, $\delta_H = t_{onH}/T_H$ high frequency (PWMH) duty cycle, P_p = pulse peak power, P_{avg} = pulse average power.

generation modulates a higher frequency PWM ($F_{P_{WMH}}$) used for anode current control. The switching transformer has been modified according to Faraday's law, based on the $F_{P_{WMH}}$ value, power supply voltage value and core parameters. We define the operational efficiency range of the microwave radiation as 1% to 100% of the magnetron output power, independent of the PWML frequency value in (5):

$$O_{ef} = 100 \cdot \delta_L \text{ [%]} \quad (5)$$

Considering the transformer power transfer without loss, the average secondary power resulted is defined by (6).

$$P_{avg} = O_{ef} P_p \quad (6)$$

The pulse peak power P_p controlled by δ_H through the energy transferred into the step-up transformer (4) is an average power (7) of the high frequency t_{onH} pulses during the t_{onL} time and creates a proportional microwave power:

$$P_p = \frac{1}{N \cdot t_{onH}} \int_0^{N t_{onH}} e(t) \cdot i(t) dt \quad (7)$$

```

/*10mS(100Hz) event with 40MHz clock /4 = 10.000.000 instructions
/100Hz = 100.000 = 01_86_A0*/
/*define registers: */
time_lo = 01h, time_mid=86h, time_hi=A0h, time_reg,
modulation_period = 100, bres_lo, bres_mid, bres_hi,
operational_efficiency
/*define IO: PWML is IO pin */
/*define other routines: PWMH is high frequency PWM routine*/

/*initialize:*/ time_reg = modulation_period
bres_lo = time_lo
bres_mid = time_mid + 1
bres_hi = time_hi
/*interrupt service routine start*/
define local: interrupt_exit,
save W_register, save status_register
test bres_mid = 0 ?
yes, decrement bres_hi
no, decrement bres_mid
test bres_mid = 0 ?
no, goto interrupt_exit
yes, test bres_hi = 0 ? /*both mid & hi = 0?*/
no, goto interrupt_exit
yes, /*event occur, reload registers:*/
bres_hi = time_hi
bres_mid = time_mid
bres_lo = bres_lo + time_lo /*cumulate the error*/
test bres_lo overflow?
no, bres_mid = bres_mid + 1
yes, /*event action:*/
time_reg = time_reg - 1
test time_reg = 0?
yes, time_reg = modulation_period /*initialize time_reg*/
no,
interrupt_exit: reset TMR0 interrupt flag
time_reg = modulation_period ?
yes, PWML = on, PWMH on
no, time_reg = modulation_period - operational_efficiency?
yes, PWML = off, PWMH off
no,
restore status_register, restore W_register
return from interrupt
/*interrupt service routine end*/

```

Figure 9. Zero error interrupt service routine, pseudo-code.

where $N = t_{onL}/T_H = \delta_L \cdot T_L/T_H$ is the number of high frequency pulses during t_{onL} and $e(t)$, $i(t)$ are the pulse voltage amplitude and current pulse respectively.

The dual modulated PWM is implemented with Bresenham's zero error algorithm [13] using timer 0 (TMR0) for $F_{P_{WML}}$ generation, and the compare-capture-PWM module (CCP) of the microcontroller for $F_{P_{WMH}}$ generation.

The firmware was tested into an embedded system, custom designed around the PIC18F44J11 microcontroller. The code generates an event at every 10mS using 40MHz clock frequency. The interrupt service routine is described as pseudo-code in (Fig. 9) and should be read as normal flow: only one of the conditional branches may be satisfied once, the other passes the flow to the next pseudo-code instruction. Since the oscillator frequency of the microcontroller can not be divided without error to get 10.00 mS period, Bresenham algorithm allows the alternation of two imperfect time periods to produce an average which match any ideal period.

```

/*route the PWMH channel output to IO pin*/
unlock PPS write control
/* PWM output A routed to pin_RP20:*/
RPOR20 = CCP1_P1A
lock PPS write control
pin_RP20_direction = output
/*PWMH frequency/duty-cycle configuration start*/
/*config PWM period:*/
set PR2 register
/* config PWM duty_cycle:*/
set CCPR1L register
set CCP1CON bit [5,4]
/*config TMR2 prescaler:*/
set T2CON
/*config CCP for PWM operation:*/
set CCP1CON bit [3-0]
/*PWMH frequency/duty-cycle configuration end*/

/*PWMH on, routine start*/
CCP1CON bit [3-0] = 0b1100
/*PWMH on, routine end*/

/*PWMH off, routine start*/
CCP1CON bit [3-0] = 0b0000
/*PWMH off, routine end*/

```

Figure 10. High frequency PWM generation, pseudo-code.

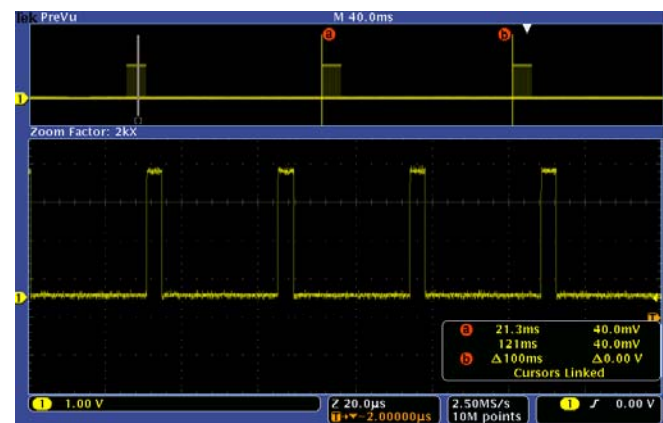


Figure 11. Dual PWM screenshot, upper: PWML=10Hz, 10%, bottom: zoom image of PWMH =29KHz, 11%.

The Bresenham computed delay value is stored in a 24bit variable (three bytes) where the last significant byte is keeping the positive or negative error on every occurred event. The described interrupt routine (Fig. 9) allows generating of zero error $F_{P_{WML}}$ in the range of 0.4Hz to 50Hz. The high frequency PWM ($F_{P_{WMH}}$) routine pseudo-code is described in (Fig. 10).

V. MODIFIED INVERTER CHARACTERISTICS

The modified inverter keeps the power switching structure from (Fig. 6) unaltered, with essential hardware modifications on the driving and protection circuitry side. The transformer TR2 was added for continuous filament heating of the magnetron (3.3V/10A). TR2 matches the isolation requirements since its secondary voltage has the same potential as the anodic voltage. The protection and driver circuitries (Fig. 12, A) are using fast comparators for sensing the voltage and current of Q1 during switching and ultra-fast optocouplers interfacing with the driving embedded system. The modified inverter uses a combined protection circuit, the hardware loop (A) which controls a current limiting device (C) and the software loop, which controls the input signal generation on S1-1 and follows the feedback on S1-2. The inverter's hardware closed loop is faster (around 250nS) than the software loop implemented in the embedded system which drives the inverter. The feedback signal on S1-2 is active high only when either the current or the voltage on the main switch Q1 is higher than recommended values.

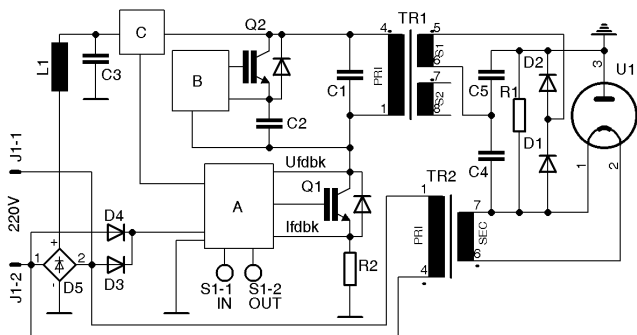


Figure 12. Modified ZVC structure, software pattern controlled: A-protection and driver circuitry, B-forming and driver circuitry, C-current limiting circuit.

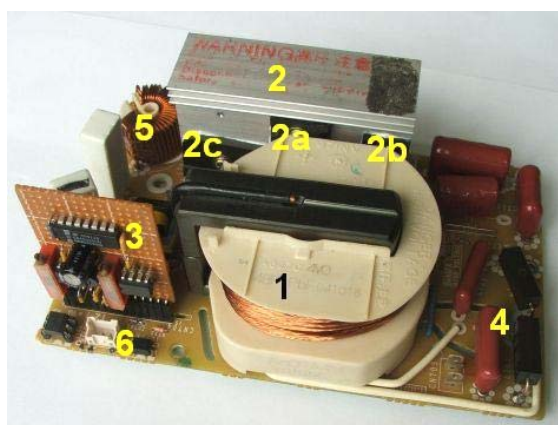


Figure 13. Modified inverter appearance: 1-step-up transformer, 2-heatsink: 2a-main switch, 2b-subswitch, 2c-bridge, 3-protection and driver circuitry, 4-voltage doubler, 5-DC smoothing filter, 6-embedded system driving connector.

The protection circuit (A) was implemented experimentally on a PCB prototype board (3, Fig. 13) maintaining the pinout compatibility of the inverter's motherboard with the original daughter-card driver replaced by it.

After the embedded system was set with a fixed operational efficiency range of 100%, the high frequency duty cycle (PWMH) has been varied in the range 10-40% and the output parameters of the inverter were measured using the experimental setup from (Fig. 14). The output power versus PWMH duty cycle has a linear variation on the entire driving range (Fig. 15), while the output inverter voltage is constant rather the PWMH duty cycle.

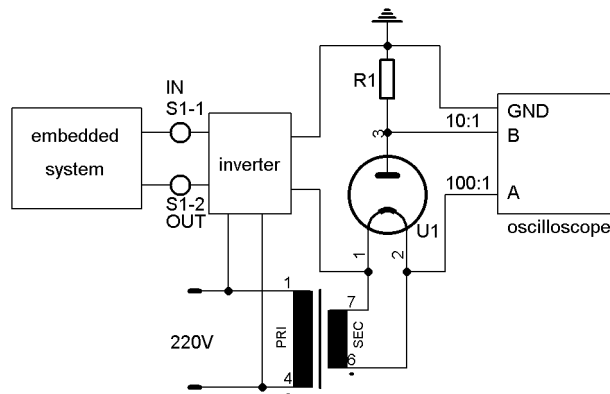


Figure 14. The experimental measurement setup.

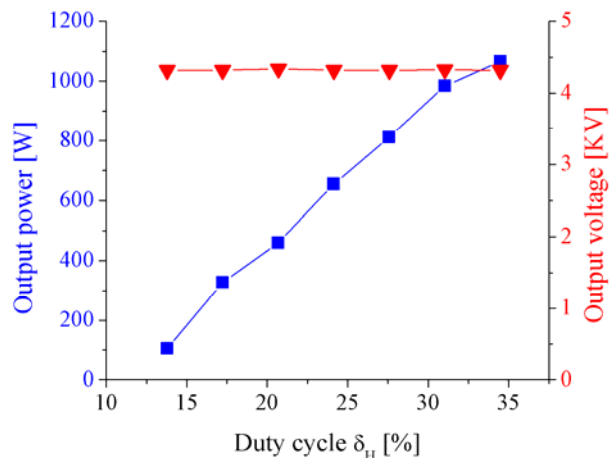


Figure 15. Inverter output characteristic, experimental result.

The experimental setup chain (Fig. 16) used for measuring the microwave generator spectrum is based on an Agilent E4402B spectrum analyzer (5) connected to the waveguide (2a) of the microwave generator (2) through a directional coupler (2a) and a variable attenuator (4).

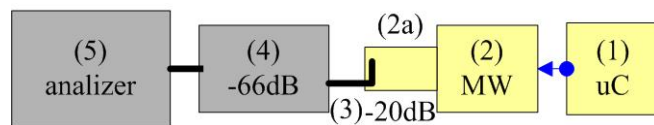


Figure 16. Experimental setup for microwave spectrum measurement: 1-embedded system, 2-microwave generator, 2a-waveguide, 3-directional coupler, 4-variable attenuator, 5-spectrum analyzer.

The magnetron is driven by our custom embedded system [12] using the modified inverter (Fig. 13). The magnetron output power value was software-set to approx. 125W and the peak power was measured on the spectrum analyzer (Fig. 17). The measured pulse pack bandwidth is 70MHz, about 15% larger than observed on conventional CW magnetron spectrum.

The ripple voltage of the inverter power supply adds a modulation of the microwave pulses (Fig. 17) due to the magnetron passing between the continuous oscillating area to the off-cycle area and backward.

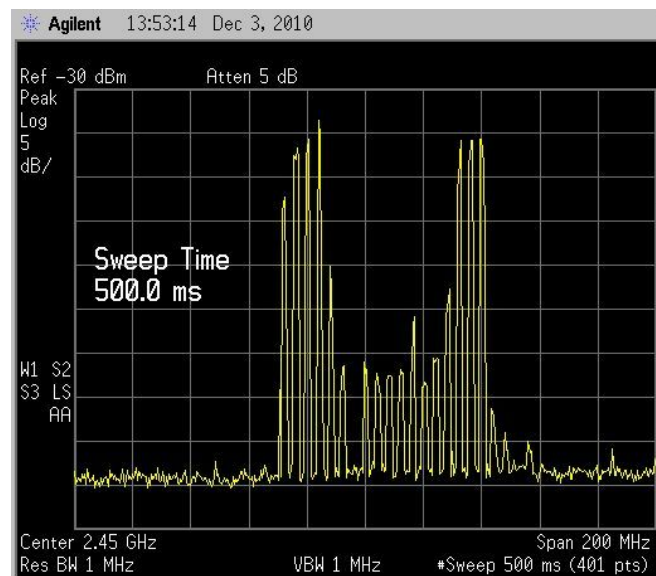


Figure 17. The microwave spectrum at the generator output: center frequency 2450MHz, span 200MHz, maximum generator pulse amplitude -35dBm (measured amplitude) +86dB (total attenuation), whole pulses bandwidth 70MHz.

VI. CONCLUSIONS

Driving a ZVS inverter with a pattern modulation entirely software-generated from an auxiliary embedded system is a delicate task, mainly because the firmware is dedicated to multiple time-consuming tasks (temperature measurement, RTC generation, communication, data storage, etc.). Designing protective circuits for the power section, which is running under heavy switching conditions (current pulses up to 50A at 800V on the main switch), is mandatory. Since an embedded system firmware may exhibit random bottlenecks, unexpected delays in the program flow or even parasitic glitches on the IO pins, maintaining the inverter in the safe operating area is very important. On the other hand, the software pattern generated by the firmware is reflected in the output inverter parameters, so a complete validation process of the firmware [14] is also necessary. The method presented here allows a large range of microwave power variation (100W-1200W) and energy variation (1% to 100% of any programmed power value, with variable period) at

the CW magnetron output, being as far as we know a novel method for supplying a CW magnetron and obtaining short microwave pulses. The complexity of our proposed and tested solution is entirely compensated by the advantage of obtaining fine software-controlled pulses of microwave radiation, as required by medical treatments or other processes in scientific and industrial applications. The pattern can be configured for the generation of both fixed and variable frequency PWM, allowing the usage of the method for driving other inductive load devices as well.

REFERENCES

- [1] V. Surducan, E. Surducan, R. Ciupa, "Medical and scientific apparatus with microwave thermal and non-thermal effect" *Nonconventional Technology Review*, Nr. 1, pp.42-49, 2010, [Online]. Available: <http://www.revtn.ro/no1-2010.html>.
- [2] P. Vecchia, R. Matthes, G. Zieglerberger, J. Lin, R. Saunders, A. Zwerdlow, "Exposure to high frequency electromagnetic fields, biological effects and health consequences (100KHz-300GHz)" pp.4, ICNIRP 16/2009 [Online]. Available: www.icnirp.de/documents/RFReview.pdf.
- [3] R. Narita, H. Kako, H. Imamura, *Magnetron Drive Apparatus*, patent US4858095, 1989, [Online]. Available: www.freepatentsonline.com/4858095.html.
- [4] E. Surducan, V. Surducan, "Procedeu si instalatie pentru procesarea dinamica a substantei in camp de microunde de putere" patent RO 00122063, 2008 [Online]. Available: <http://bd.osim.ro/cgi-bin/invsearch8>.
- [5] A. W. Hull, "The magnetron" *Journal of the American Institute of Electrical Engineers*, vol. 40, no. 9, pages 715-723, September 1921.
- [6] H. E. Hollman "Magnetron" *US patent 2123728*, in Germany: November 29 1935, in USA: July 12, 1938 [Online]. Available: <http://patft.uspto.gov/netahtml/PTO/patimg.htm>.
- [7] Ghe. Rulea, "Tehnica frecvențelor foarte înalte" Editura Tehnica București 1966, pp323, pp334.
- [8] D. Bessyo et al "High frequency heating apparatus" US patent 6362463 B1, 2002 [Online]. Available: www.freepatentsonline.com/6362463.html.
- [9] E. Miyata, S. Hishikawa, K. Matsumoto, M. Nakaoka, D. Bessyo, K. Yasui, I. Hirota, H. Omori, "Quasi-resonant ZVS PWM Inverter-fed DC-DC Converter for Microwave Oven and its Input Harmonic Current Evaluations", *Industrial Electronics Society, 1999. IECON '99 Proceedings. The 25th Annual Conference of the IEEE* [Online]. Available: <http://dx.doi.org/10.1109/IECON.1999.816498>.
- [10] D. Bessyo, K. Yasui, M. Nakaoka, "A method of Decreasing the Harmonic Distorsion for Inverter Microwave Oven", *Electronics and Communications in Japan*, part1, vol.85, no.4, pp.1528-1537, 2002 [Online]. Available: <http://dx.doi.org/10.1002/ecja.1087>.
- [11] M. Ishitobi, S. Moisseev, L. Gamage, M. Nakaoka, D. Bessyo, H. Omori, "Pulse Width and Pulse Frequency Modulation Pattern Controlled ZVS Inverter Type AC-DC Power Converter with Lowered Utility AC Grid Side Harmonic Current Components for Magnetron Drive", *Power Electronic Specialists Conference, Cairns, Qld., Australia*, pp 2062-2066, IEEE 2002 [Online]. Available: <http://dx.doi.org/10.1109/PSEC.2002.1023118>.
- [12] V. Surducan, E. Surducan, R. Ciupa, M. Roman, "Embedded system controlling microwave generators in hyperthermia and diathermy medical devices", *IEEE International Conference on Automation, Quality and Testing, Robotics 2010*, pp.366-371, ISBN978-1-4244-6722-8, Cluj-Napoca, Romania, [Online]. Available: <http://dx.doi.org/10.1109/AQTR.2010.5520705>.
- [13] R. Black, "Zero error-1second timing" [Online]. Available: http://www.romanblack.com/one_sec.htm.
- [14] IEC60601-1-4, Medical electrical equipment, Part 1-4: General requirements for safety. Programmable medical electrical systems.